Kinetic H/D/T Isotope and Solid State Effects on the Tautomerism of the Conjugate Porphyrin Monoanion

Jürgen Braun,[1a] Reinhard Schwesinger,[1b] Philip G. Williams,[1c] Hiromi Morimoto,[1c] David E. Wemmer,[1c] and Hans-Heinrich Limbach*,[1a]

Contribution from the Institut für Organische Chemie, der Freien Universität, Berlin, Takustrasse 3, D-14195 Berlin, Germany, the Institut für Organische Chemie, der Universität Freiburg i. Br., Albertstrasse 21, D-79104 Freiburg, F.R.G., and the National Tritium Labelling Facility, Lawrence Berkeley National Laboratory, One Cyclotron Road, Berkeley, California 94720

Received April 22, 1996[⊗]

Abstract: Using dynamic NMR spectroscopy, the kinetic isotope effects of the degenerate single hydron transfer in the conjugate ^{15}N-labeled porphyrin anion Por-H$^-$ dissolved in organic solvents have been measured as a function of temperature. Por-H$^-$ was generated by dissolving the labeled parent compound porphyrin together with the phosphazene base 1,1,1,5,5,5-hexakis(dimethylamino)-3-[(1,1,2,2-tetramethylpropyl)imino]-3-[[tris(dimethylamino)-phosphoranyliden]amino]-1λ^5,3λ^5,5λ^5,1,4-triphosphazadiene (*t*Hept-P_4) in organic solvents. In addition, by reaction of porphyrin with the base 1,1,1,5,5,5-tetrakis[tris(dimethylamino)phosphoranylidene]amino]phosphonium fluoride ($P_5^+F^-$) Por-H$^-$ could be embedded into the solid state and its tautomerism followed by ^{15}N CPMAS NMR. Surprisingly, within the margin of error, the degeneracy of the tautomerism was not lifted in the solid state and the rate constants of the proton transfer were identical in the liquid and the solid. The kinetic isotope effects at 240 K (extrapolated) are given by $k^H/k^D = 34$ and $k^H/k^T \approx 152$. The size and the temperature dependence of the isotope effects indicates a proton tunneling mechanism as in the parent porphyrin where this process is nondegenerate. However, the proton tunneling contribution is much larger in the anion as there the process is degenerate. These findings are reproduced in terms of a modified Bell tunnel model for both systems.

Introduction

The degenerate double proton transfer in porphyrin (Por-H_2, Figure 1a) and its derivatives has been a matter of intense experimental[2−7] and theoretical[8,9] studies in the past two decades. This tautomerism has been found by NMR to take place in the liquid[2,3,4e] as well as in the solid state, where its degeneracy may be lifted, when certain substituents are introduced.[4,5] The tautomerism of porphyrin can also be induced both by visible[6] and by IR-light.[7] Various approaches have been made in order to calculate the reaction energy surface[8] that indicate a stepwise reaction mechanism as depicted in Figure 1a; moreover, as *ab initio* calculation methods have been improved, the calculated barrier energies[8e] have substantially decreased and are now of the order of those found experimentally.[4e] Progress has also been made in the measurement and interpretation of kinetic HH/HD/DD isotope effects of double proton transfer reactions.[9−12] These effects have recently been determined using dynamic ^{1}H NMR of unsubsti-

⊗ Abstract published in *Advance ACS Abstracts,* October 1, 1996.

(1) (a) Freie Universität Berlin. (b) Lawrence Berkeley National Laboratory.

(2) (a) Storm, C. B.; Teklu, Y. *J. Am. Chem. Soc.* **1972**, *94*, 1745. (b) Storm, C. B.; Teklu, Y. *Ann. N.Y. Acad. Sci.* **1973**, *206*, 631. (c) Abraham, R. J.; Hawkes, G. E.; Smith, K. M. *Tetrahedron Lett.* **1974**, 1483. (d) Abraham, R. J.; Hawkes, G. E.; Smith, K. M. *J. Chem. Soc. Perkin Trans. 2* **1974**, 1483. (e) Yeh, H. J. C.; Sato, M.; Morishima, I. *J. Magn. Reson.* **1977,** *99*, 365. (f) Gust, D.; Roberts, J. D. *J. Am. Chem. Soc.* **1977,** *99*, 3637. (g) Irving, C. S.; Lapidot, A. *J. Chem. Soc., Chem. Commun.* **1977,** 184. (h) Limbach, H. H.; Hennig, J. *J. Chem. Soc., Faraday 2* **1979,** *75*, 752. (i) Limbach, H. H.; Hennig, J.; Gerritzen, D.; Rumpel, H. *Faraday Discuss. Chem. Soc.* **1982,** *74*, 822. (j) Hennig, J.; Limbach, H. H. *J. Magn. Reson.* **1982,** *49*, 322. (k) Eaton, S. S.; Eaton, G. R. *J. Am. Chem. Soc.* **1977,** *99*, 1601. (l) Stilbs, P.; Moseley, M. E. *J. Chem. Soc., Faraday 2* **1980,** *76*, 729. (m) Stilbs, P. *J. Magn. Reson.* **1984,** *58*, 152. (n) Hennig, J.; Limbach, H. H. *J. Am. Chem. Soc.* **1984,** *106*, 869. (o) Crossley, M. J.; Harding, M. M.; Sternhell, S. *J. Am. Chem. Soc.* **1986,** *108*, 3608. (p) Crossley, M. J.; Field, L. D.; Harding, M. M.; Sternhell, S. *J. Am. Chem. Soc.* **1987,** *109*, 2335.

(3) (a) Schlabach, M.; Wehrle, B.; Limbach, H. H.; Bunnenberg, E.; Knierzinger, A.; Shu, A. Y. L.; Tolf, B. R.; Djerassi, C. *J. Am. Chem. Soc.* **1986,** *108*, 3856. (b) Schlabach, M.; Limbach, H. H.; Bunnenberg, E.; Shu, A. Y. L.; Tolf, B. R.; Djerasssi, C. *J. Am. Chem. Soc.* **1993,** *115*, 4554. (c) Schlabach, M.; Rumpel, H.; Limbach, H. H. *Angew. Chem.* **1989,** *101*, 84; *Angew. Chem., Int. Ed. Engl.* **1989,** *28*, 78. (d) Schlabach, M.; Scherer, G.; Limbach, H. H. *J. Am. Chem. Soc.* **1991,** *113*, 3550.

(4) (a) Limbach, H. H.; Hennig, J.; Kendrick, R. D.; Yannoni, C. S. *J. Am. Chem. Soc.* **1984,** *106*, 4059. (b) Limbach, H. H.; Wehrle, B.; Schlabach, M.; Kendrick, R. D.; Yannoni, C. S. *J. Magn. Reson.* **1988,** *77*, 84. (c) Schlabach, M.; Wehrle, B.; Braun, J.; Scherer, G.; Limbach, H. H. *Ber. Bunsenges. Phys. Chem.* **1992,** *96*, 821. (d) Wehrle, B.; Limbach, H. H.; Köcher, M.; Ermer, O.; Vogel, E. *Angew. Chem.* **1987,** 99, 914; *Angew. Chem., Int. Ed. Engl.* **1987,** 26, 934. (e) Braun, J.; Schlabach, M.; Wehrle, B.; Köcher, M.; Vogel, E.; Limbach, H. H. *J. Am. Chem. Soc.* **1994,** *116*, 6593. (f) Kendrick, R. D.; Friedrich, S.; Wehrle, B.; Limbach, H. H.; Yannoni, C. S. *J. Magn. Reson.* **1985,** *30*, 159.

(5) (a) Frydman, L.; Olivieri, A. C.; Diaz, L. E.; Valasinas, A.; Frydman, B. *J. Am. Chem. Soc.* **1988,** *110*, 5651. (b) Frydman, L.; Olivieri, A. C.; Diaz, L. E.; Frydman, B.; Morin, F. G.; Mayne, C. L.; Grant, D. M.; Adler, A. D. *J. Am. Chem. Soc.* **1988,** *110*, 336. (c) Frydman, L.; Olivieri, A. C.; Diaz, L. E.; Frydman, B.; Kustanovich, I.; Vega, S. *J. Am. Chem. Soc.* **1988,** *111*, 7001. (d) Frydman, L.; Rossomando, P. C.; Sambrotta, L.; Frydman, B. *J. Phys. Chem.* **1992,** *96*, 4753.

(6) (a) Völker, S.; van der Waals, J. H. *Mol. Phys.* **1976,** 32, 1703. (b) Voelker, S.; Macfarlane, R. *IBM Res. Dev.* **1979,** *23*, 547.

(7) (a) Butenhoff, T.; Moore, C. B. *J. Am. Chem. Soc.* **1988,** *110*, 8336. (b) Butenhoff, T.; Chuck, R. S. Limbach, H. H.; Moore, C. B. *J. Phys. Chem.* **1990,** *94*, 7847.

(8) (a) Almlöf, J. *Int. J. Quant. Chem.* **1974,** *8*, 915. (b) Kusmitsky, V. A. Solovyov, K. N. *J. Mol. Struct.* **1980,** *65*, 219. (c) Merz, K. M.; Reynolds, C. H. *J. Chem. Soc. Chem. Commun.* **1988,** 90. (d) Merz, K. M.; Reynolds, C. H. *J. Chem. Soc., Chem. Commun.* **1988,** 90. (e) Reimer, J. R.; Lü, T. X.; Crossley, M. J.; Hush, N. S. *J. Am. Chem. Soc.* **1995,** *117*, 2855.

(9) (a) Limbach, H. H.; Hennig, J. *J. Chem. Phys.* **1979,** *71*, 3120. (b) Limbach, H. H.; Hennig, J.; Stulz, J. *J. Chem. Phys.* **1983,** *78*, 5432. (c) Sarai, A. *J. Chem. Phys.* **1982,** *76*, 5554. (d) Sarai, A. *J. Chem. Phys.* **1984,** *80*, 5431. (e) Limbach, H. H. *J. Chem. Phys.* **1984,** *80*, 5343. (f) Bersuker, G. I.; Polinger, V. Z. *Chem. Phys.* **1984,** *86*, 57. (g) Smedarchina, Z.; Siebrand, W.; Wildman, T. A. *Chem. Phys. Lett.* **1988,** *143*, 395. (h) Smedarchina, Z.; Siebrand, W.; Wildman, T. A. *Chem. Phys.* **1983,** *78*, 5432.

S0002-7863(96)01313-3 CCC: $12.00

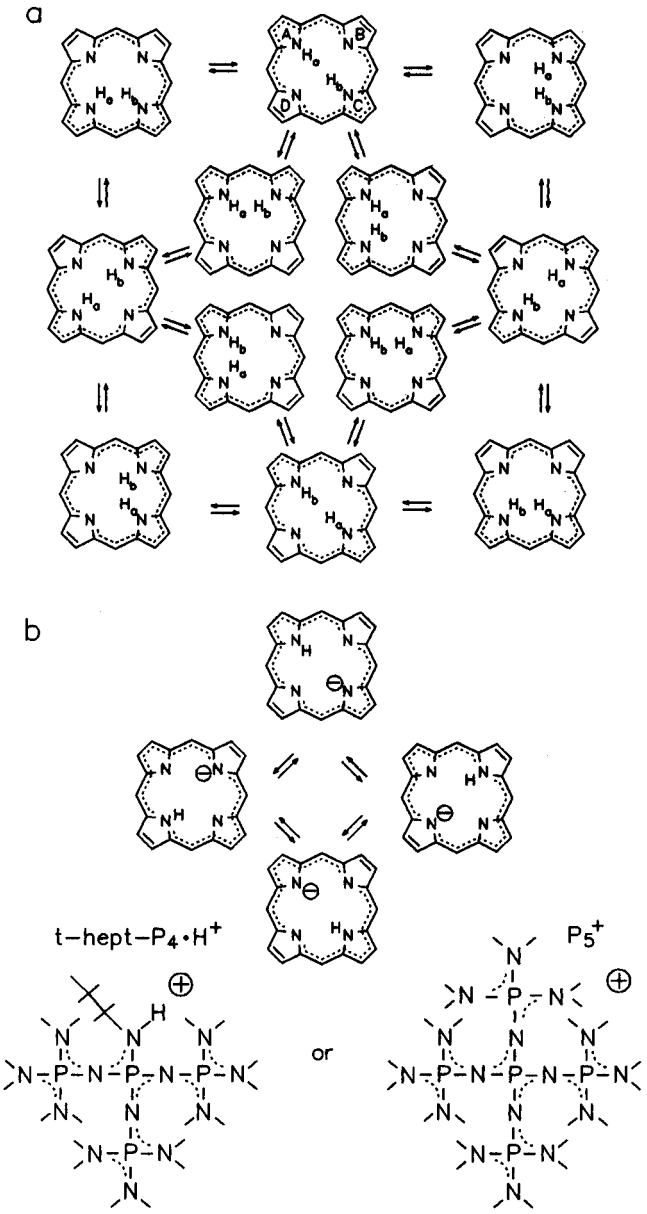

Figure 1. (a) Stepwise tautomerism of porphyrin. The subscripts a and b of the mobile protons symbolize their individual nuclear spin state. (b) Tautomerism of the conjugate porphyrin monoanion and chemical structures of the counterions used.

tuted ^{15}N-labeled porphyrin dissolved in organic liquids as well as for the polycrystalline compound using ^{15}N cross polarization, magic angle spinning (CPMAS) NMR spectroscopy.[4e] They support the stepwise mechanism, where the hydron (H, D, T) in flight produces a primary kinetic isotope effect. Possible secondary kinetic isotope effects produced by the hydron at rest—transferred in the second step—could not be observed. The theoretical description of the reaction dynamics of the tautomerism has also improved in the past years.[4e,7,9] The main result of these studies is that the reaction takes place at low temperature by thermally activated tunneling, but a minimum energy is necessary for the tunnel process to occur corresponding mainly to the energy of the metastable cis intermediates included in Figure 1 and partly to some reorganization energy of the porphyrin skeleton. However, the quality of the experimental data was not yet sufficient in order to distinguish between different tunneling models.

Recently, two advancements have been made in this field which will further improve our understanding of the mechanism of proton transfer in a cavity as the porphyrin skeleton. The first was the use of ^{3}H NMR spectroscopy (tritium = ^{3}H or T) for measuring rate constants of the triton transfer in porphyrin.[13] Although ^{3}H NMR had previously been used to follow triton transfer reactions,[14] the extension of this approach to measure kinetic H/T isotope effects by combined ^{1}H and ^{3}H NMR line shape analysis had not yet been reported. As with other NMR applications of tritium, this may be because tritium is radioactive and some additional sample preparation and handling precautions are required. The kinetic H/D/T isotope effects on the first single hydron transfer step in porphyrin (Figure 1a) measured at various temperatures were large and supported the idea of a thermally activated proton tunnel mechanism even at room temperature.

A second advancement was the finding that strong bases can remove a single proton from the parent compound porphyrin leading to the conjugate porphyrin anion Por-H$^-$ [15] previously thought to be unstable.[16] Moreover, the intramolecular degenerate tautomerism depicted in Figure 1b could be detected by NMR as well as some rate constants determined by line shape analysis.

The choice of the base was a critical point. Conventional inorganic bases immediately form metalloporphyrins such as Por-M$^-$ [M]$^+$ or Por-M,[17] meaning that neutral organic bases B are required that must be strong enough to remove an inner proton of Por-H$^-$. In addition, the structure of the base should be such that intermolecular proton transfer between BH$^+$ and Por-H$^-$ is so slow that no measurable NMR line shape effects arise. We found that higher phosphazene bases such as 1,1,1,5,5,5-hexakis(dimethylamino)-3-[(1,1,2,2-tetramethylpropyl)imino]-3-[[tris(dimethylamino)phosphoranylidene]amino]-1λ^5,3λ^5,5λ^5-1,4-triphosphazadiene (*t*Hept-P$_4$) or the salt 1,1,1,5,5,5,-tetrakis[[dimethylamino)phosphoranylidene]amino]-phosphonium fluoride (P$_5^+$F$^-$) (Figure 1b) were suitable.[15] The syntheses and properties of phosphazene bases have been described recently, including the X-ray crystal structure[18d] of P$_5^+$F$^-$.

(10) Limbach, H. H. Dynamic NMR Spectroscopy in the Presence of Kinetic Hydrogen Deuterium Isotope Effects. In *NMR Basic Principles and Progress*; Springer-Verlag: Berlin 1991; Vol. 26, Chapter 2.

(11) (a) Limbach, H. H.; Seiffert, W. *J. Am. Chem. Soc.* **1980,** *102*, 538. (b) Gerritzen, D.; Limbach, H. H. *J. Am. Chem. Soc*. **1984,** *106*, 869. (c) Meschede, L.; Gerritzen, D., Limbach, H. H. *Ber. Bunsenges. Phys. Chem*. **1988,** *92*, 469. (d) Limbach, H. H.; Meschede, L.; Scherer, G. *Z. Naturforsch.* **1989,** *44A*, 459. (e) Meschede, L.; Limbach, H. H. *J. Phys. Chem.* **1991,** *95*, 10267.

(12) (a) Otting, G.; Rumpel, H.; Meschede, L., Scherer, G.; Limbach, H. H. *Ber. Bunsenges. Phys. Chem.* **1986,** *90*, 1122. (b) Rumpel, H.; Limbach, H. H.; Zachmann, G. *J. Phys. Chem*. **1989,** *93*, 1812. (c) Rumpel, H.; Limbach, H. H. *J. Am. Chem. Soc.* **1989,** *111*, 5429. (d) Scherer, G.; Limbach, H.-H. *J. Am. Chem. Soc*. **1989,** *111*, 5946; **1989,** *111*, 5946. (e) Scherer, G.; Limbach, H. H. *J. Am. Chem. Soc.* **1994,** *113*, 1230. (f) Scherer, G.; Limbach, H. H. *Croat. Chim. Acta* **1994,** *67*, 431.

(13) Braun, J.; Limbach, H. H.; Williams, P.; Morimoto, H.; Wemmer, D. *J. Am. Chem. Soc*. **1996**, *118*, 7231.

(14) (a) Dixon, R. E.; Williams, P. G.; Saljoughian, M.; Long, M. A.; Streitwieser, A. *Magn. Reson. Chem.* **1991,** *29*, 509. (b) Morimoto, H.; Williams, P. G., *Fusion Technol.* **1992,** *21*, 256.

(15) Braun, J.; Hasenfratz, C., Schwesinger, R., Limbach H. H. *Angew. Chem.* **1994,** *106*, 2302; *Angew. Chem., Int. Ed. Engl*. **1994,** *33*, 2215.

(16) (a) Knop, J. V.; Knop, A. *Z. Naturforsch*. **1970,** *A25*, 1720; (b) **1970,** *A25*, 1726.

(17) Arnold, J.; Dawson, D. Y.; Hoffman, C. G. *J. Am. Chem. Soc.* **1993,** *115*, 2707.

(18) (a) Schwesinger, R.; Hasenfratz, C.; Schlemper, H.; Walz, L.; Peters, E. M.; Peters, K.; von Schnering, H. G. *Angew. Chem.* **1993,** *105*, 1420; *Angew. Chem., Int. Ed. Engl.* **1993,** *32*, 1361. (b) Schwesinger, R.; Schlemper, H. *Angew. Chem*. **1987,** *99*, 1212; *Angew. Chem., Int. Ed. Engl*. **1987,** *26*, 1167. (c) Schwesinger, R., *Nachr. Chem. Tech. Lab*. **1990,** *38*, 1214. (d) Hillebrecht, H.; Wenzl, P.; Schwesinger, R., unpublished. See also: Schwesinger, R.; Link, R.; Thiele, G.; Rotter, H.; Honert, D.; Limbach, H. H.; Männle, F. *Angew. Chem*. **1991,** *103*, 1376; *Angew. Chem., Int. Ed. Engl.* **1991,** *30*, 1372.

In this paper we report on the full kinetic H/D/T isotope effects of the tautomerism of the conjugate porphyrin anion (Figure 1b), obtained by using a combination of ^{1}H and ^{3}H NMR of partially deuterated or tritiated ^{15}N-labeled Por-H$^-$. In addition, the conjugate porphyrin anion could be incorporated into the solid $P_5^+F^-$ salt (Figure 1b) where its tautomerism was followed by variable-temperature ^{15}N CPMAS NMR spectroscopy.

After the Experimental Section and the presentation of the results, the kinetic H/D/T isotope and solid state effects on the tautomerism are discussed in comparison with those of the parent compound porphyrin.

Experimental Section

Synthesis of the ^{15}N-Labeled Conjugate Porphyrin Anion. In a first stage, the ^{15}N-labeled parent compound porphyrin was synthesized from $^{15}NH_4Cl$ (95% ^{15}N enriched, Chemotrade, Leipzig) as described previously[4e] using slightly modified versions of the procedures described for the unlabeled compounds.[19] In order to produce the anion, the parent compound was dissolved in tetrahydrofuran together with a 2-fold excess of *t*Hept-P_4 or the $P_5^+F^-$ salt leading to

$$\text{Por-H}_2 + t\text{Hept-P}_4 \rightleftarrows \text{Por-H}^- + t\text{Hept-P}_4\cdot\text{H}^+ \quad (1)$$

$$\text{Por-H}_2 + 2\text{P}_5^+\text{F}^- \rightleftarrows [\text{P}_5]_2^{2+}\text{Por-H}^-[\text{FHF}]^- \quad (2)$$

We found that the solubility of the anion in tetrahydrofuran is much higher than the solubility of the parent compound. Furthermore, the higher solubility results in a considerable melting point depression of the solutions prepared, as compared to the pure liquid. Finally, when Por-H$^-$ is exposed to humid air, water, or other proton donors the parent compound is formed again. Therefore, all operations concerning Por-H$^-$ had to be carried out in a glovebox or a vacuum line.

Preparation of NMR Samples. The NMR samples were prepared as described previously[4e,10] on a vacuum line. The solvent, deuterated tetrahydrofuran (THF-d_8) was dried and stored over potassium−sodium/anthracene. All other solvents used in the syntheses were dried over molecular sieve, 3 Å.

Preparation of Partially Deuterated NMR Samples. Several samples were prepared according to the following procedure. In the case of sample 1, solid [$^{15}N_4$]porphyrin (3 mg) was placed into an NMR tube equipped with a Teflon needle valve attached to the vacuum line and dried for 1 h *in vacuo* at 10^{-7} mbar. The partial deuteration of porphyrin was achieved as described previously:[4e] 1 mL of a mixture of 50% D_2O and 50% H_2O was condensed on the solid by vacuum transfer. The lower part of the sealed tube was then heated for 7 days to 120 °C and the water removed *in vacuo*. This procedure was repeated once. In a glovebox under argon atmosphere (water content less than 2 ppm) a 2-fold excess of *t*Hept-P_4 was added into the NMR tube which was immediately evacuated at the vacuum line. Finally, 0.5 mL of dried THF-d_8 was added and the tube flame-sealed. During this procedure the contents were kept at 77 K. By NMR, the final deuterium fraction in the mobile hydron sites of the conjugate porphyrin anion was found to be 35%.

Sample 2 was prepared in a similar way, but nonlabeled porphyrin was used as a precursor.

Preparation of Tritiated NMR Samples. In the first stage we tritiated the parent compound [$^{15}N_4$]porphyrin as described previously.[13] A saturated solution of 3 mg of this compound dissolved in dichloromethane was transferred via a syringe into a 25 mL flask attached to a vacuum line. The flask contained 0.2 mg of freshly prepared, approximately 65% enriched T_2O, introduced by vacuum transfer.[14b] After 10 min stirring, the liquids were removed *in vacuo*. In order to remove any residual water, the porphyrin was again dissolved in dry dichloromethane which was removed in the same way. This procedure was repeated twice.

In a glovebox, a 2-fold excess of the *t*Hept-P_4 base was dissolved in dry THF and transferred using a syringe on the tritiated solid porphyrin; the solution stirred for 3 min and then was transferred into an NMR tube. After attaching the latter to the vacuum line and removing the dissolved gases by several cycles of freeze−pump cycles, the tube was flame-sealed. The degree of tritiation was determined by NMR line shape analysis as described below.

Preparation of a Sample for Optical Spectroscopy. The samples for optical spectroscopy were prepared in a way similar to the NMR samples, using a quartz cell (Hellma, Müllheim, Germany) to which a Teflon needle valve was attached for handling on the vacuum line.

Preparation of a Solid Sample of $[P_5]_2^{2+}$[Por-H]$^-$[FHF]$^-$ for Variable-Temperature ^{15}N CPMAS NMR Spectroscopy. As solid $[P_5]_2^{2+}$[Por-H]$^-$[FHF]$^-$ is very hygroscopic, sample 3 for ^{15}N CPMAS NMR was prepared as follows. To a glass insert for 7 mm NMR rotors (Wilmad) was attached a Teflon needle valve for vacuum operations. In the glovebox, 20 mg of solid [$^{15}N_4$]porphyrin and a 2-fold excess of $P_5^+F^-$ were placed in the glass insert, which was then attached to the vacuum line. Subsequently, 5 mL of dry THF was added by vacuum transfer, leading to the product according to eq 2. The solvent was then evaporated and the solid transferred into the glass insert by rinsing the inner glass surfaces repeatedly by cooling the outer glass surfaces with liquid nitrogen. Finally, the insert was flame-sealed, during which time the contents were kept at 77 K. The decomposition of a small amount of the sample part could not be avoided.

Spectroscopic Measurements. The optical spectra were measured using a Shimadzu-UV240 UV spectrometer and a Shimadzu-RF540 fluorescence spectrometer. Liquid state ^{1}H NMR measurements on samples 1 and 2 were performed on a Bruker NMR spectrometer AMX 500 (500 MHz) and additional ^{1}H and the ^{3}H NMR measurements on a Bruker NMR spectrometer AMX 300 (320 MHz). The ^{15}N CPMAS NMR experiments were carried out at 9.12 MHz on a Bruker CXP 90 MHz spectrometer equipped with a standard 7 mm Doty MAS probe using the pulse sequence of Torchia[20] proposed for solid state T_1 measurements. During the equilibration period where the magnetization created by cross polarization is stored along the static magnetic field, spin diffusion takes place between protonated and nonprotonated nitrogen atoms, which helps to reduce signal intensity distortions arising from site-dependent cross polarization dynamics when magnetization transfer arising from proton exchange is very slow.[4b] For the variable-temperature MAS experiments, a home-built temperature controller was employed as described previously.[4f] The sample temperatures were controlled using PT 100 resistance thermometers; a temperature increase arising from spinning[21] could be neglected at the spinning speeds employed. The NMR spectra were calculated using home-written programs for personal computers based on procedures described previously.[10,22]

Results

Results of the Dynamic NMR Experiments. In this section we report the results of the variable-temperature liquid and solid state dynamic NMR experiments performed on the conjugated porphyrin anion. The ^{1}H NMR signals of the counterion *t*Hept-P_4 H$^+$ were not analyzed.

(a) Line Shape Analyses of the Inner Proton and Triton Signals of the Conjugate Porphyrin Anion in the Liquid State. The rate constants of the proton transfer k^H in the conjugate porphyrin anion were determined by analysis of the variable-temperature NMR signals of the inner proton in Por-H$^-$ dissolved in THF-d_8 using sample 1, the preparation of which is described above. The superposed experimental and calculated signals obtained at 500 MHz are depicted in Figure 2a. The signals appear around −2.7 ppm, which is typical for porphyrins; for comparison, the corresponding signals of the

(19) (a) Silverstein, R. M.; Ryskiewicz, E. E.; Chaikin, S. W. *J. Am. Chem. Soc*. **1954,** *76*, 4485. (b) Longo, R. R.; Thorne, E. J.; Adler, A. D.; Sym, S. *J. Heterocycl. Chem.* **1975,** *12*, 1305.

(20) Torchia, D. *J. Magn. Reson.* **1978,** *30*, 613.

(21) Wehrle, B.; Aguilar-Parilla, F.; Limbach, H. H. *J. Magn. Reson*. **1990,** *87*, 584; **1990,** *87*, 592.

(22) (a) Binsch, G. *J. Am. Chem. Soc.* **1969,** *91*, 1304. (b) Ernst, R. R.; Bodenhausen, G.; Wokaun, A. *Principles of Nuclear Resonance in One and Two Dimensions*; Clarendon Press: Oxford, 1987.

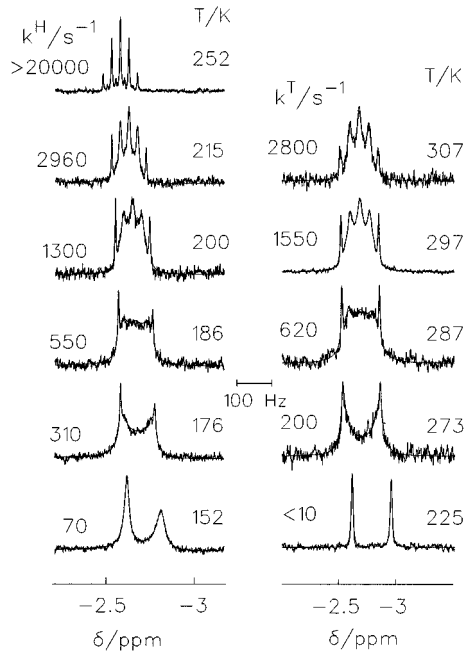

Figure 2. Superposed experimental and calculated variable-temperature high-field NMR signals of the inner hydrons of the conjugate [$^{15}N_4$]-porphyrin anion Por-L$^-$, L = H, T, with *t*Hept-P_4-H$^+$ as a counter-cation. (a, left) ^{1}H NMR signals of sample 1 containing 65% Por-H$^-$ and 35% Por-D$^-$ dissolved in THF-d_8 at a concentration of ~0.015 M; 500 MHz, 65° pulses, duration 6.5 μs, 9 kHz spectral width, 3.5 s repetition time, up to 600 scans; adapted from ref 15. (b, right) ^{3}H NMR signals of sample 4 containing 10% Por-T$^-$ dissolved in THF-h_8; 320 MHz, 5 μs 60° pulses, 8 kHz spectral width, 3.6 s repetition time, number of scans between 200 and 1400 below 250 K and up to 10 000 above 290 K.

parent compound appear at −3.5 ppm.[4e] A direct comparison is difficult, however, as the chemical shifts strongly depend on association and on the solvent. As in the case of the parent compound, at low temperature a doublet is observed arising from scalar coupling with the attached ^{15}N nucleus, indicating a slow exchange of the proton between the nitrogen sites. The coupling constants $^1J_{^1H-^{15}N}$ are similar to those of the parent compound[4e] and decrease slightly with increasing temperature from 101 Hz at 145 K to 98.5 Hz at 235 K, as indicated in Table 1 of the standard Supporting Information. A differential line broadening of the ^{1}H−^{15}N doublet is observed at low temperature and arises from a reduced molecular mobility and an interference between the ^{1}H−^{15}N dipolar interaction and the chemical shift anisotropy.[23] As temperature is increased, rotational diffusion becomes faster and the asymmetry disappears. At the same time, a doublet−pentet transition is observed at about 200 K arising from a fast intramolecular proton transfer between all four nitrogen atoms. We note that the temperature of the doublet−pentet transition is much higher, i.e., around 250 K in Por-H_2, which indicates that the tautomerism becomes much faster by removing one proton from porphyrin. The observation of the pentet is proof for an intramolecular reaction pathway of the tautomerism. The line shape analysis was carried out in a similar way as described previously for Por-H_2[4e] and leads to the rate constants k^H. k^H is the inverse average lifetime of the proton in a given nitrogen site until either a clockwise or counterclockwise jump to an adjacent nitrogen site occurs, characterized by equal probabilities. No evidence for direct jumps to opposite nitrogen sites was obtained by line shape analysis as such a process would induce a change of the inner proton signal from a doublet at low to a triplet at high temperature.[3] In order to obtain k^H by line shape analysis the value of the line width W_o in the absence of exchange is needed. This quantity can be derived at higher temperatures from the line width of the outer signal components. At low temperatures, where only an exchange-broadened doublet is observed, this procedure is not practicable. Here, the signals were simulated by using the values of k^H obtained from the carbon-bound proton signals as described below, adapting W_o for the high- and the low-field doublet components.

In a similar way, the NMR signals of the inner triton of sample 4 were measured and analyzed by ^{3}H NMR and the rate constants k^T of the triton transfer determined. The results of the line shape analyses are illustrated in Figure 2b. There is a slight difference in the chemical shifts of the inner proton and deuteron, but this difference arises from small concentration variations. The coupling constant $^1J_{^3H-^{15}N}$ decreases slightly from a value of 109.5 Hz at 225 K and to 105.4 Hz at 307 K (see standard Supporting Information). The doublet−pentet transition temperature is substantially higher for the triton as compared to the proton, indicating a large kinetic H/T isotope effect on the tautomerism.

(b) Line Shape Analyses of the Aromatic Proton Signals of the Conjugate Porphyrin Anion and Its Deuterated Analog in the Liquid State. As described in the following, the rate constants k^H and k^D could be determined without systematic errors by line shape analysis of the signals of the carbon-bound protons of samples 1 and 2 at deuterium fractions of about 35%. Sample 2 contained the partially deuterated non-^{15}N-enriched porphyrin anion. By comparison of the two samples, homonuclear proton−proton and heteronuclear proton−nitrogen couplings could easily be distinguished, because in the nonlabeled sample, ^{14}N quadrupole relaxation is so fast that the scalar heteronuclear interactions to ^{14}N are averaged. The signals of several carbon-bound protons were larger for the ^{15}N-

Table 1. Rate constants k^L (L = H, D, T) of the Tautomerism of the Conjugate Porphyrin Anion Determined by NMR Line Shape Analysis

	k^H/s^{-1}		k^D/s^{-1}		k^D/s^{-1}	k^T/s^{-1}
T/K	liquid	solid	liquid	*T*/K	liquid	liquid
158		110[c]		241	90[a]	
168	200[b]			243	100[b]	
171	245[a]			247	140[a]	
173	290[b]			249	200[b]	
176	310[a]			252	260[a]	
181	400[a]			255	350[b]	
186	550[a]			257	360[a]	
190	730[a]			259	440[b]	
195	950[a]			262	600[a]	
197	1100[b]			268	850[a]	
199		1000[c]		269	1000[b]	
200	1300[a]			273		200[d]
205	1700[a]			281	2400[a]	
208	1950[b]			287		620[d]
215	2960[a]		10[a]	297		1550[d]
218	3500[b]	2900[c]	11[a]	307		2800[d]
226	5400[a]		24[a]			
230	6250[b]		35[a]			
235	8400[b]		47[a]			
236			60[a]			
238		11000[c]	68[b]			

[a] Sample 1: see Figures 2a, 3, and 4, deuterium fraction of 35% in the inner proton sites. [b] Sample 2: non-^{15}N-labeled, deuterium fraction of 50% in the inner proton sites. [c] Sample 3: see Figure 5. [d] Sample 4: see Figure 2b, ^{15}N-labeled, tritium fraction of 10% in the inner proton sites; solvent, THF-h_8.

(23) (a) Shimidzu, H. *J. Chem. Phys.* **1964,** *40*, 3357. (b) Rüterjans, H.; Kaun, E.; Hull, W. E.; Limbach, H. H. *Nucleic Acids Res.* **1982,** 10, 7027. (c) Griffey, R. H.; Poulter, C. D.; Aamaizumi, Z.; Nishimura, S.; Hurd, R. E. *J. Am. Chem. Soc.* **1982,** *104*, 5811. (d) Gueron, M.; Leroy, J. L.; Griffey, R. H. *J. Am. Chem. Soc.* **1983,** *105*, 7262.

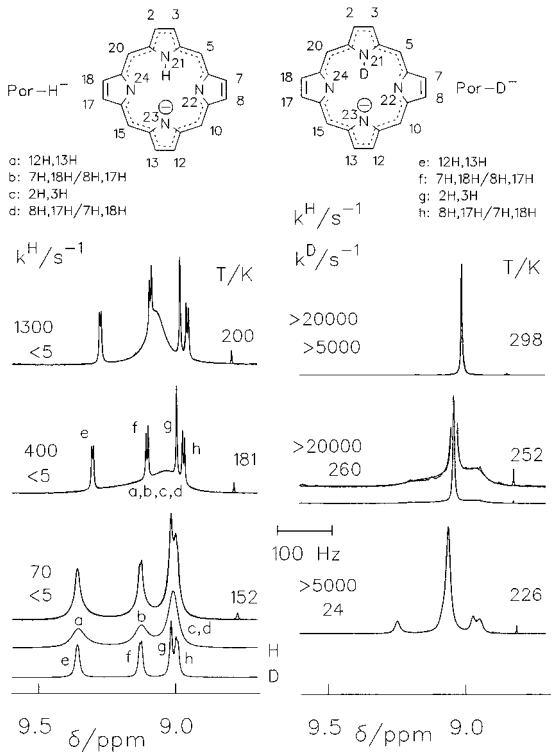

Figure 3. Superposed experimental and calculated variable-temperature ^{1}H NMR signals of the β-pyrrole protons of Por-H$^-$ (65%) and Por-D$^-$ (35%) in sample 1. For experimental details see Figure 2. Half-width in the absence of exchange between 2 and 6 Hz, mainly arising from unresolved couplings with ^{15}N as corroborated by NMR measurements on unlabeled sample 2 (not shown).

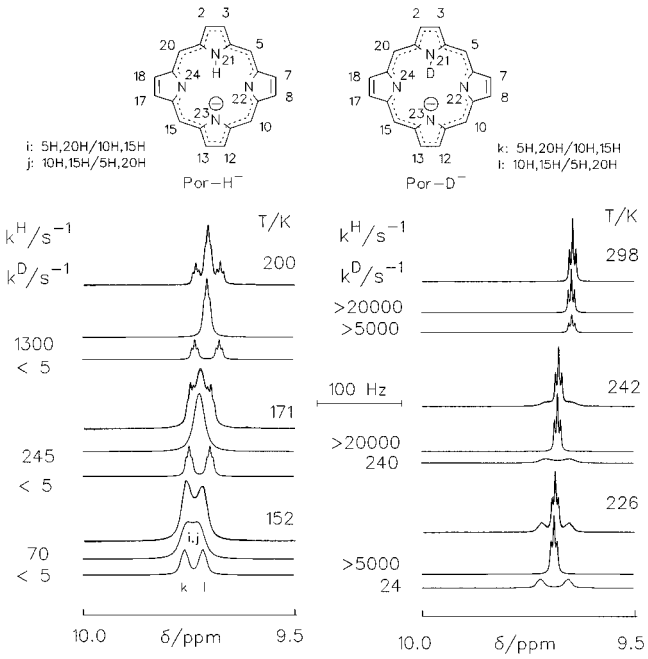

Figure 4. Superposed experimental and calculated variable-temperature ^{1}H NMR signals of the methine protons of Por-H$^-$ (65%) and Por-D$^-$ (35%) in sample 1. For experimental details, see Figure 2.

labeled anion as compared to the nonlabeled anion attributed to small unresolved ^{1}H−^{15}N couplings. Finally, we note that the values of k^D cannot be determined by analysis of the ^{2}H NMR of the central deuteron because of its short transverse relaxation times caused by the quadrupole moment and the small coupling constant $^1J_{^2H-^{15}N}$. Therefore, the H/D kinetic isotope effects were determined by line shape analysis of the carbon-bound proton signals as described in the following.

Figure 3 depicts the superposed experimental and calculated variable-temperature signals of the β-pyrrole protons. Since the anion was deuterated to about 35%, we observe two signal sets, a−d for Por-H$^-$ and e−h for Por-D$^-$ at about $\nu_a = \nu_e = 9.15$ ppm, $\nu_b = \nu_f = 9.04$ ppm, $\nu_c = \nu_g = 8.93$ ppm, and $\nu_d = \nu_h = 8.90$ ppm. The two sets are best separated at 181 K, where the signals a−d are already coalesced because of the fast proton transfer in Por-H$^-$, but where the signals e−h are still sharp, indicating that the rate constants k^D of the deuteron transfer at this temperature are small.

The signals f and g are split into doublets as expected for the proton pair 7H/8H and the equivalent pair 17H/18H. The splitting therefore corresponds to the coupling constants $^3J_{eff} = {}^3J_{7H8Hf} = {}^3J_{17J18H} = 4.2$ Hz. However, the assignment of signals f and g to the two protons within a pair was not established in this study. The assigment of signal a to 2H/3H and of d to 12H/13H was based on the observation in the parent compound that the chemical shifts of β-pyrrole protons in the nitrogen protonated pyrrole units appear at higher field as compared to the nonprotonated ones and that the heteronuclear coupling constant $^1J_{^1H-^{15}N}$ is larger. This interaction clearly leads to a doublet splitting of 4.1 Hz of signal e, in contrast to signal h where the coupling is not resolved. Thus, signals a−h clearly establish the formation and the structure of the conjugate porphyrin anion.

As temperature is increased above 181 K, the signals a−d first coalesce into a single sharp line followed by signals e−h. As temperature is decreased below 181 K, all signals broaden slightly because of the shortening of the transverse relaxation time arising from slow molecular tumbling. The contribution of k^D to the line widths of signals e−h, i.e., $k^D/\pi \ll 1$ Hz, is small as compared to the total line width of a few hertz. Therefore, from these signals, the line width W_o in the absence of exchange was determined and used to obtain k^H by simulation of signals a−d, which could still be distinguished from signals e−h, as shown in the subspectra corresponding to 152 K in Figure 3. Thus, the values of k^H obtained from signals a−d in the temperature range between 150 and 210 K where signals e−h do not exhibit line-broadening are not affected by systematic errors. At higher temperatures, the exchange broadening of signals a−d is so large that the value of W_o does not influence particularly the line shapes in contrast to the chemical shifts of signals a−d, which could be obtained from signals e−h up to 235 K. Above this temperature, the exchange broadening of the coalesced lines a to d was so small that W_o could be determined again from this signal and used to determine k^D by the analysis of signals e−h. Here, the values of the chemical shifts were extrapolated from the low-temperature range between 150 and 230 K, assuming linear dependencies well fulfilled at low temperatures (see standard Supporting Information).

Finally, it is interesting to discuss the line shapes of the methine proton signals of sample 1 depicted in Figure 4. Again, at low temperatures two signal sets i, j and k, l are observed for Por-H$^-$ and Por-D$^-$ (see calculated subspectra) because in contrast to Por-H$_2$, the methine protons are no longer equivalent. An assignment of the signals to the proton positions 5H/20H or to 10H/15H could, in principle, be obtained by various NMR experiments but was beyond the scope of this kinetic study. Signals k and l in the 200 K spectrum are clearly split into triplets arising from scalar coupling to the two adjacent ^{15}N atoms, where $^3J_{5H21N} \approx {}^3J_{5H22N} \approx {}^3J_{20H24N} \approx {}^3J_{10H22N} \approx {}^3J_{15H24N} \approx {}^3J_{10H23N} \approx {}^3J_{15H23N} \approx 4.5$ Hz. At lower temperatures, line broadening resulting from a shortening of the transverse

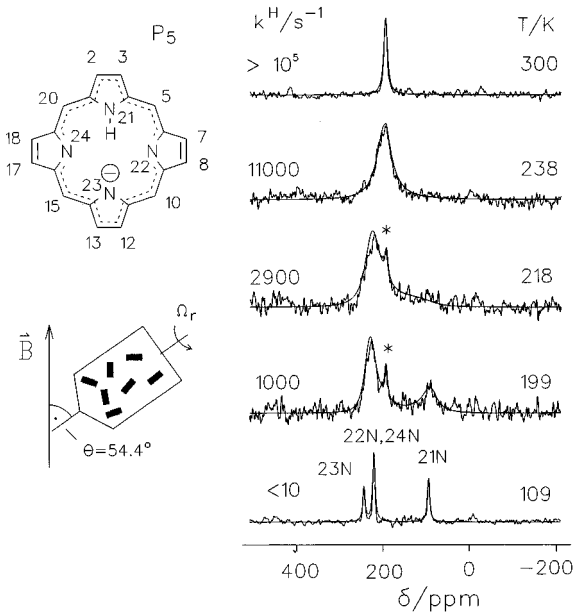

Figure 5. Superposed experimental and calculated variable-temperature ^{15}N CPMAS NMR spectra of a of Por-H$^-$ embedded in solid $P_5^+F^-$ (sample 3): 9.12 MHz, 3−9 ms CP times, 7 kHz spectral width, 3.3 s repetition time, 1.9−2.2 kHz spinning speed. The peak labeled with an asterisk arises from an impurity formed during flame-sealing of the rotor glass insert. For further description, see text.

relaxation times was again observed. Since the H/D isotope effects on the chemical shifts are minimal, i.e., $\nu_k \approx \nu_i$ and $\nu_j \approx \nu_l$ rate constants k^H could be determined at low temperatures with high accuracy from signals i and j, by obtaining the chemical shifts and line widths in the absence of exchange from signals k and l. In addition, at higher temperatures, some values of k^D could also be derived as long as they were of the order of the chemical shift difference $\nu_k - \nu_j = 0.084$ ppm $\hat{=}$ 42 Hz. The scalar heteronuclear coupling survives at high temperatures, giving rise to triplet splittings of the coalesced signals.

(c) Variable-Temperature ^{15}N CPMAS NMR Studies of the Tautomerism of the Conjugate Porphyrinanion in Solid $[P_5]_2^{2+}$[Por-H]$^-$[FHF]$^-$. These measurements were performed in order to evaluate possible cation−anion or other interactions which could perturb the tautomerism of Por-H$^-$. The experiments were performed on sample 4, the preparation of which was described in the Experimental Section.

The superposed experimental and calculated 9.12 MHz (2.1 T) ^{15}N CPMAS NMR spectra of sample 4 containing $[P_5]_2^{2+}$[Por-H]$^-$[FHF]$^-$ are depicted in Figure 5. Due to the small magnetic field applied, spinning speeds of between 1.9 and 2.2 kHz were sufficient to suppress the rotational side bands. At low temperatures, three singlets are observed, characterized by the chemical shifts $\nu_{23N} = 251$ ppm, $\nu_{22N} = \nu_{24N} = 228$ ppm, and $\nu_{21N} = 99$ ppm with respect to $^{15}NH_4Cl$ and the relative intensities of about 1:2:1. The assignment to the nitrogen positions is straightforward. As temperature is increased, all lines broaden and coalesce, indicating a rapid tautomerism also in the solid state. Moreover, at high temperatures only one single line is observed, indicating that the tautomerism renders all nitrogen atoms equivalent. In other words, the gas phase and liquid state degeneracy of the tautomerism is not lifted in solid $[P_5]_2^{2+}$[Por-H]$^-$[FHF]$^-$. We assign the signal labeled by an asterisk to an impurity formed by flame-sealing of the NMR rotor glass insert described in the Experimental Section. The line shape analysis was carried out in the usual way by setting up the appropriate line shape equations of intramolecular exchange. The line width in the absence of exchange was taken from the spectrum at 109 K and the chemical shifts kept constant within the whole temperature range.

Table 2. Summary of Kinetic Results of the Proton Transfer in Porphyrin and Its Conjugate Anion[a]

L	log A^L	E_a^L	T_{min}	T_{max}		240 K	298 K		240 K	298 K
					Porphyrin					
H	10.7	37.2	209	290	k^H	410	15600	k^H/k^D	34	11.4
D	11.6	48.5	240	320	k^D	12	1370	k^D/k^T	4.4	3.4
T	12.8	51.5	275	320	k^T	2.7	404	k^H/k^T	152	39
					Porphyrin Anion					
H	7.8	17.7	158	238	k^H	8360	10^5	k^H/k^D	93	16.5
D	11.3	43	215	281	k^D	90	6100	k^D/k^T	12.2	3.0
T	12.8	55	273	307	k^T	7.4	2030	k^H/k^T	1140	49.6

[a] Frequency factors A^L in s^{-1}, activation energies E_a^L in kJ mol^{-1}, k^L rate constants of single-proton transfer in s^{-1}; T_{min}, T_{max}, temperature range where rate constants were determined. The calculation of kinetic isotope effects is partly based on rate constants extrapolated in terms of the modified Bell tunneling model. The parameters for the parent porphyrin are taken from ref 13.

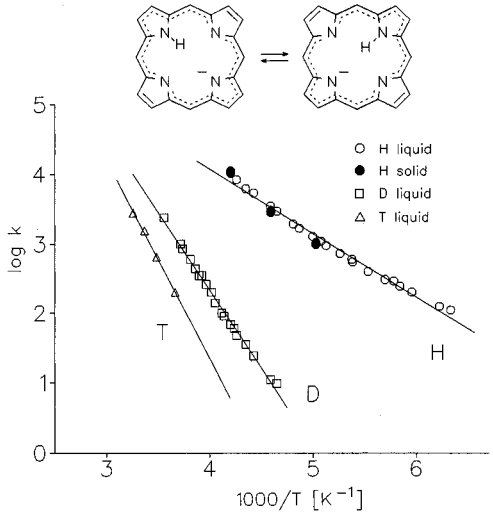

Figure 6. Arrhenius diagram of the H, D, and T transfer in the conjugate porphyrin anion evaluated by dynamic NMR. The open symbols stem from THF solutions with *t*Hept-P_4-H$^+$ as a countercation, and the solid symbols are from Por-H$^-$ in the solid state (sample 3). The solid lines were calculated by linear regression (parameters see Table 2).

(d) Summary of Kinetic Results. All rate constants obtained are summarized in Table 1. Activation parameters obtained by linear regression assuming Arrhenius relations are listed in Table 2, together with those obtained previously for the tautomerism of the parent compound porphyrin. The Arrhenius diagram obtained is depicted in Figure 6.

Optical spectroscopy of the conjugate porphyrin anion

The changes in the UV/visible and fluorescence spectra upon deprotonation of Por-H_2, reported in ref 15, are illustrated in Figure 7. The spectra of Por-H_2 (Figure 6a,b) have been measured and discussed previously.[16,24] The transition of lowest energy (Q_x band, $S_o \rightarrow S_1^x$ appearing for Por-H_2 at 615 nm is

(24) (a) Gamgee, A. *Z. Biol.* **1897,** *34*, 505. (b) Gouterman, M. *J. Chem. Phys.* **1959,** *30*, 1139. (c) Gouterman, M. *J. Chem. Phys.* **1960,** *33*, 1523. (d) Gouterman, M. *J. Mol. Spectrosc.* **1961,** *6*, 138. (e) Abraham, R. J. *Mol. Phys.* **1961,** *4*, 145. (f) Kuhn, H.; Huber, W. *Helv. Chim. Acta* **1959,** *42*, 363. (g) Longuet-Higgins, H. C.; Rector, C. W.; Platt, J. R. *J. Chem. Phys.* **1950,** *18*, 1174. (h) Seely, G. R. *J. Chem. Phys.* **1957,** *27*, 125. (i) Falk, J. E. *Porphyrins and Metalloporphyrins*; Elsevier; Amsterdam, 1964. (j) Gouterman, M.; Khalil, G. E. *J. Mol. Spectrosc.* **1974,** *53*, 88. (k) Rawlings, D. C.; Davidson, E. R., Gouterman, M. *Theor. Chim. Acta* **1982,** *61*, 227.

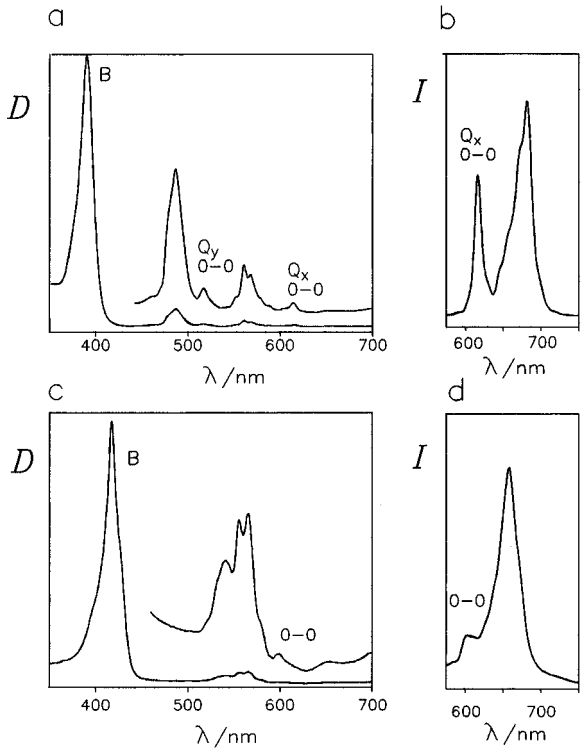

Figure 7. (a) Room-temperature UV/visible and (b) fluorescence spectra of Por-H_2 dissolved in THF, excitation wave length 570 nm. (c and d) corresponding spectra of Por-H^-/*t*Hept-P_4·H^+ in THF. *D*, optical density; *I*, intensity. Adapted from ref 15.

shifted in Por-H^- to 600 nm (Figure 6c). The appearance of the 0−0 transition at 600 nm for Por-H^- is confirmed by the fluorescence data shown in Figure 6d, obtained at an excitation wavelength of 570 nm. No evidence of a calculated bathochromic shift beyond 700 nm could be found, but in contrast, the Soret band of Por-H_2 at 390 nm is shifted to 420 nm in the conjugate anion and is more intensive. In addition, major spectral changes are observed in the region between 480 and 580 nm. In order to estimate the pK_a of free acid porphyrin, a titration experiment of the more soluble octaethylporphyrin (OEP) with 3-(*tert*-butylimino)-1,1,1,5,5,5-hexakis(dimethylamino)-3-[[tris(dimethylamino) phosphoranyliden]amino]-1λ^5,3λ^5,5λ^5-1,4-triphosphazadiene (*t*But-P_4) was performed. The deprotonation of OEP was followed by the analysis of the Soret band shift. At concentrations of 0.01 M *t*But-P_4 in dry tetrahydrofuran, OEP was deprotonated to approximately 85% at room temperature. From this result we extrapolate in a similar way as described previously[18b] for OEP an absolute pK_a value of 37−38 in acetonitrile. For the parent compound Por-H_2, we expect a slightly higher acidity, i.e., a pK_a value of about 35−36.

Discussion

We have shown that the conjugate porphyrin anion Por-H^- is a stable species in the liquid and the solid state and can be obtained by treatment of the parent compound with strong large organic phosphazene bases (Figure 1b), under anhydrous conditions. The UV/visible and fluoresence spectra of Por-H^- were characterized and exhibit interesting differences from the parent compound porphyrin Por-H_2. The structure of the anion was also proved by NMR at low temperatures, where all proton resonances could be assigned. Ongoing optical and NMR studies not reported here show that the formation of a conjugate anion is not only a property of Por-H_2 but that anions are also formed by substituted porphyrins such as octaethylporphyrin (OEP) and mesotetraphenylporphyrin (TPP). The absolute pK_a values of porphyrins in acetonitrile were estimated to be of the order of 37.

It was shown by NMR that the conjugate porphyrin anion is subject to a degenerate intramolecular tautomerism according to Figure 1b. Fortunately, the added phosphazene bases and their protonated analogs did not catalyze the intermolecular proton transfer of the anion to an observable extent, which could have complicated the evaluation of the kinetic data of the intramolecular tautomerism by dynamic NMR. Therefore, the full kinetic H/D/T isotope effects of the tautomerism could be evaluated by a combination of liquid state ^1H and ^3H NMR spectroscopy of the ^{15}N-labeled anion in a fairly large temperature interval. Additional high-resolution solid state ^{15}N NMR experiments on the anion embedded in the solid $P_5^+F^-$ (Figure 1b) revealed that the degeneracy of the tautomerism is not lifted in the solid state and that the rate constants of the proton tautomerism in the liquid and the solid state coincide. The kinetic data obtained were summarized in Tables 1 and 2. The resulting combined Arrhenius diagram of the tautomerism was depicted in Figure 6, where the solid lines were calculated as described below. Semiempirical calculations using the AM1 method integrated in the MOPAC 6.0 program package[25] were performed in order to obtain a rough idea about the reaction energy surface of the tautomerism of the conjugate porphyrin anion. The reaction pathway of the proton between two adjacent nitrogen atoms was linear with a saddle point exhibiting an energy of 151 kJ mol L^{-1}. A direct proton transfer between two opposite nitrogen atoms involved a hilltop exhibiting an energy of 298 kJ mol L^{-1}. Naturally, these energies are unreal because of the number of approximations used.

In this section, we first address the mechanism of the formation of Por-H^- and then the effects of the environment on the tautomerism of Por-H^- . The main part of this section is, however, devoted to a discussion of the kinetic H/D/T isotope effects and the mechanism of the tautomerism of the conjugate porphyrin anion and of the parent compound.

Mechanism of the Formation of the Conjugate Porphyrin Anion. The conjugate anion of porphyrin was prepared according to eqs 1 and 2. In the first case, the driving force is the basicity of *t*Hept-P_4 to which one proton of Por-H_2 is transferred. This reaction and the corresponding back-reactions are so slow, i.e., probably in the second time scale, as no line-broadening arising from intermolecular proton exchange of the conjugate porphyrin anion could be detected. Intermolecular proton exchange would lead to a loss of the scalar coupling of the remaining inner proton with the ^{15}N nuclei, in contrast to the findings of Figure 2. The low rate of the proton transfer between the two reactants can be explained by a very remote location of the mobile proton in the countercation. A direct transfer therefore seems impossible, and probably hydrogen-bonded complexes of one or two water molecules with *t*Hept-P_4 are essential as catalyst for the proton transfer to occur. However, because of the efforts to exclude water from the samples and the excess of the base, the concentration of such complexes must be small.

In the case of the $P_5^+F^-$ salt, the cation is not directly involved in the reaction according to eq 2. The strong base is the "naked" fluoride anion,[18d] which removes a porphyrin proton producing the stable $[FHF]^-$ anion. Here, it is conceivable that two F^- ions directly attack porphyrin and that the reaction is faster, but the back-reaction should also be slow because of the stability of $[FHF]^-$, which also prevents intermolecular proton exchange of Por-H^-.

(25) Stewart, J. J. P. *QCPE No. 455*, Indiana University, Bloomington, IN 47405.

Structure of the Polycrystalline Conjugate Porphyrin Anion Salt. The determination of the structure of the solid formed by porphyrin and $P_5^+F^-$ was beyond the scope of this study, but some information was obtained indirectly by high-resolution solid state ^{15}N NMR. As discussed above, the salt $[P_5]_2^{2+}[Por\text{-}H]^-[FHF]^-$ is probably formed according to eq 2 although we cannot exclude the formation of the salts $P_5^+Por\text{-}H^-$ and $P_5^+[FHF]^-$ either as a physical mixture or as solid solutions, possibly also including unreacted salt $P_5^+F^-$. However, as the exact structure of the solid did not seem relevant to us for the understanding of the tautomeric process of $Por\text{-}H^-$ in the solid state, this question was not pursued in detail.

Absence of Matrix Effects on the Tautomerism of the Conjugate Porphyrin Anion. The observations that the degeneracy of the tautomerism of $Por\text{-}H^-$ is not lifted in the solid formed with $P_5^+F^-$ and that the rate constants of the tautomerism coincide with those determined for the liquid solution—where *t*Hept-P_4 was used as countercation—are fortunate. This is because the dynamics of the tautomerism can be regarded in good approximation as independent of intermolecular interactions with surrounding molecules, their structure, ordering, and mobility. It is therefore justified to compare, in the future, the experimental kinetic data with that obtained theoretically for the isolated conjugate porphyrin anion, representing a considerable simplification. As a consequence, we only calculated the reaction energy surface of the isolated anion without exploring possible effects of surrounding counterions or solvent molecules on the tautomerism of $Por\text{-}H^-$.

This absence of major matrix effects on the tautomerism can be rationalized by discussing the shape of the separate $Por\text{-}H^-$ and P_5^+ ions. Both ions are of comparable dimension and exhibit a similar charge delocalization. Only in the case of a localized point charge in the countercation one could expect that the closest nitrogen site preferentially adopts the negative charge of $Por\text{-}H^-$ in order to minimize the Coulomb energy. This would lead to a preferential proton location on the opposite nitrogen site, leading to a lifting of the degeneracy of the tautomerism in $Por\text{-}H^-$ in the solid state. On the other hand, this argument does not hold for the fairly localized $[FHF]^-$ counterion, which is presumed to be present in the solid studied. Thus, either the salt $[P_5]_2^{2+}[Por\text{-}H]^-[FHF]^-$ is formed with the $[FHF]^-$ ion placed in such a way that the degeneracy of the tautomerism of $[Por\text{-}H]^-$ is not lifted, or the solid consisted of separate regions with $P_5^+[Por\text{-}H]^-$ and $P_5^+[FHF]^-$. Solid solutions cannot be completely excluded, but in this case we would have expected a broad distribution of equilibrium constant of the tautomerism as found previously in the case of tetraazaannulenes embedded in a glassy polymer[27a] and of amorphous phthalocyanine.[27b]

Kinetic H/D/T Isotope Effects of the Tautomerism of Porphyrin and Its Conjugate Anion. In this section it is shown that the kinetic data of the tautomerism of the conjugate porphyrin anion support hydron tunneling as the main transfer pathway as in the case of the tautomerism of the parent compound.[4e,7,9,13] Tunneling as a general pathway for proton transfer reactions was suggested long ago by Bell[28a] and generally leads to a non-Arrhenius behavior of the process studied as well as to anomalous kinetic H/D/T isotope effects.[29]

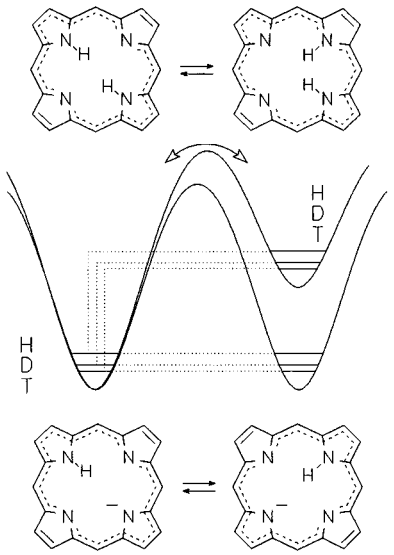

Figure 8. Comparison of the energy reaction pathways of single-proton transfers in porphyrin and its conjugate anion.

Here we will rationalize the kinetic data of the tautomerism of porphyrin and its conjugate anion in terms of the simple one-dimensional reaction profiles of Figure 8. Whereas a single-proton transfer in porphyrin is endoenergetic leading to the metastable cis intermediate, proton transfer in the isolated anion is degenerate. Within the margin of error this is also the case for the anion embedded in solid $P_5^+F^-$, as discussed above.

Let us first discuss the Arrhenius diagram of the single hydron transfer step in the parent constructed recently[13] from various experimental kinetic data,[4e,7,13] depicted in Figure 9a,b. The current, theoretically well-supported interpretation[4e,7,8,9g] of this diagram is the following: At high temperature the hydrons (H, D, T) jump over the barrier or tunnel at energies slightly below the top of the barrier. At low temperatures, however, tunneling occurs though the barrier at lower energies. The minimum energy $E_m = E_i + E_r$, where tunneling can occur is given by the energy E_i of the intermediate and a reorganization energy E_r of the skeleton preceding the tunnel process. If E_m is large, the kinetic isotope effects are greatly reduced, as shown recently for the tautomerism of oxalamidines.[12e,12f] E_m can be obtained from the slope of the Arrhenius curves at low temperature. As E_m is similar for H and D, their Arrhenius curves are in good approximation parallel at low temperature; i.e., the kinetic H/D isotope effects are then temperature independent.

A modified Bell tunneling model used to calculate the solid Arrhenius curves of Figure 9a,b has been described in detail.[4e,13] The model contains the following adjustable parameters: (i) E_m represents the minimum energy for tunneling to occur; (ii) E_d^H is the barrier height for the proton transfer at the energy E_m; (iii) the D and T transfers involve the additional barrier energies $\Delta\epsilon^{HD} = E_d^D - E_d^H$ and $\Delta\epsilon^{HT} = E_d^T - E_d^H$, with $\Delta\epsilon^{HT} = \Delta\epsilon^{HD}\,(1-3^{1/2})/(1-2^{1/2})$; (iv) $2a$ is the barrier width of the H transfer (in Å) at energy E_m; (iv) a single-frequency factor A (in s^{-1}) is used for all isotopic reactions; i.e., a possible mass dependence[28] $A^H : A^D : A^T \approx 1^{-1/2} : 2^{-1/2} : 3^{-1/2}$ is assumed to be the negligible within the margin of error; (vi) the tunneling masses $m_{eff}^L = m^L + \Delta m$, with the fixed values $m^H = 1$, $m^D =$

(26) (a) Webb, L. E.; Fleischer, E. B. *J. Chem.Phys.* **1965,** *43, 3100. (*b) Chen, B. M. L.; Tulinsky, A. *J. Am. Chem. Soc.* **1972,** *94,* 4144.

(27) (a) Wehrle, B.; .Zimmermann, H.; Limbach, H. H. *J. Am. Chem. Soc.* **1988,** *110,* 7014. (b) Wehrle, B.; Limbach, H. H. *Chem. Phys.* **1989,** *136,* 223.

(28) (a) Bell, R. P. *The Tunnel Effect*, 2nd ed.; Chapman and Hall: London, 1980. (b) Caldin, E.; Gold, V. *Proton Transfer*; Chapman and Hall: London, 1975. (c) Melander, L.; Saunders, W. H. *Reaction Rates of Isotopic Molecules*; John Wiley & Sons: New York, 1980.

(29) (a) Swain, C. G.; Stivers, E. C.; Reuwer, J. F.; Schaad, L. J. *J. Am. Chem. Soc.* **1958**, *80,* 5885. (b) Lewis, E. S.; Robinson, J. K. *J. Am. Chem. Soc.* **1968**, *90*, 4337. (c) Stern, M. J.; Western, R. E., Jr. *J. Chem. Phys.* **1974,** *60,* 2815. (d) Bell, R. P. *The Tunnel Effect*, 2nd ed.; Chapman and Hall: London, 1980; p 200. (e) Saunders, W. H. *J. Am. Chem. Soc.* **1985**, *107,* 164. (f) Cha, Y.; Murray, C. J.; Klinman, J. P. *Science* **1989**, *243,* 1325.

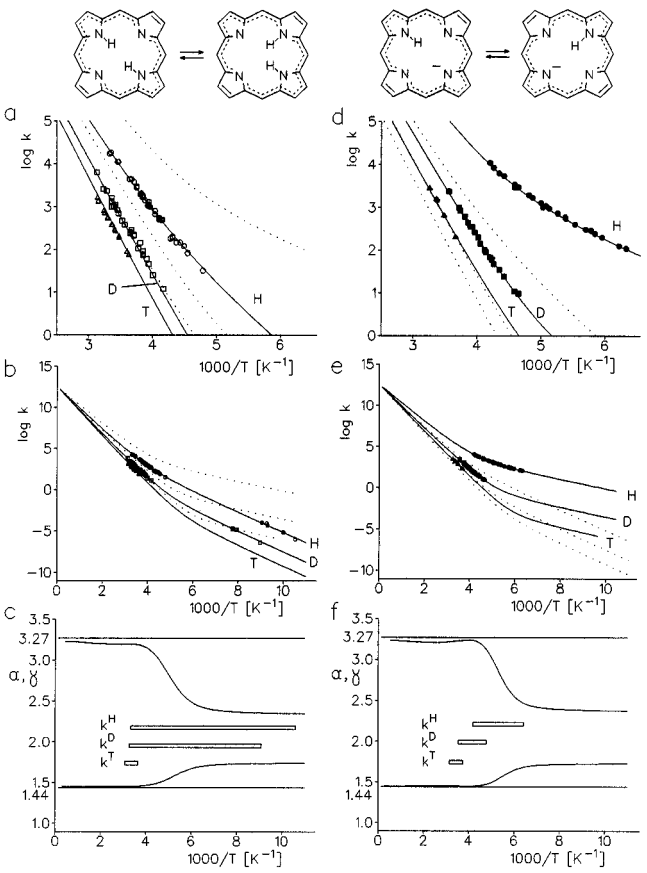

Figure 9. (a and b) Arrhenius diagram of the H, D, and T transfer in porphyrin[13] and (d and e) its conjugate anion. The solid lines were calculated in terms of the modified Bell tunneling model using the parameters of Table 3 as described in the text. The broken lines refer to the other species. (c) and (d) values of α and γ defined in eq 4 for the tautomerism of porphyrin and its conjugate anion, calculated from the theoretical Arrhenius curves. The rectangles represent the temperature range where kinetic data were obtained.

Table 3. Parameter of the Modified Bell Model of the Tautomerism of Porphyrin and Its Conjugate Anion[a]

	E_d	E_m	$E_d + E_m$	log A	$2a$	$\Delta\epsilon^{HD}$	$\Delta\epsilon^{HT}$	Δm
Por-H$^-$	34.3	10.0	44.3	12.6	0.78	7.74	11.19	1.5
Por-H$_2$	28.7	22.7	51.4	12.6	0.68	4.95	7.15	1.5

[a] Barrier height E_d and minimum energy for tunneling E_m in kJ mol^{-1}, additional barrier energy for the deuteron and the triton motion $\Delta\epsilon^{HT} = \Delta\epsilon^{HD}(1-3^{1/2})/(1-2^{1/2})$ in kJ mol^{-1}, barrier width $2a$ in Å, and frequency factor A in s^{-1}. Tunneling masses $m_{eff}^{L} = m^{L} + \Delta m$, $m^{H} = 1$, $m^{D} = 2$, and $m^{T} = 3$ (fixed).

2, and $m^T = 3$. Δm takes into account the possibility of small heavy atom displacements during the tunnel process.

The solid lines in Figure 9a,b were calculated in terms of this model via a simultaneous nonlinear least-squares fit of all three Arrhenius curves, by freely varying all parameters. The agreement between the experimental and calculated data is satisfactory. This free parameter variation was possible only by including the tritium data as they put considerable constraints on the parameter values. The resulting parameter values are listed in Table 3. Because of the unrealistic simplicity of the one-dimensional tunneling model, one should not attribute too much physical significance to these parameters. Nevertheless, these parameters are all reasonable and of the dimensions expected. The most puzzling finding was that tunneling masses of 2.5, 3.5, and 4.5 were required for reproducing the H, D, and T data, respectively. Although this could signal merely the inadequacy of the one-dimensional Bell tunneling model employed, the result is consistent with a contribution of heavy atom tunneling arising from a slight readjustment of the porphyrin skeleton during the tunneling process.

The calculated Arrhenius curves of the anion are indicated in Figure 9d,e. As the temperature range covered was smaller in the anion as compared to the parent compound, a free parameter fit was not possible for the former. Therefore, in order to calculate the Arrhenius diagram of the tautomerism of the porphyrin anion shown in Figure 9d,e, the frequency factors and the tunneling masses were taken from the parent porphyrin, assuming that these parameters should be similar. The remaining parameters could be freely adjusted. The total barrier energy $E_d + E_m$ is similar in both molecules, leading to similar overbarrier reaction rate constants and probabilities of tunneling at energies above E_m, which dominate at high temperatures. Around room temperature, the tunnel contributions are substantial and similar for D and T. The dramatic increase of the rate constants of the H transfer in the anion as compared to the parent compound arises then mainly from the circumstance that the minimum energy of tunneling E_m is smaller in the anion because the reaction is now degenerate. This increase cannot be explained in terms of an overbarrier reaction but is a criterion of tunneling.

Finally, we address the problem of expressing kinetic H/D/T isotope effects in the form

$$\alpha = \ln(k^H/k^T)/\ln(k^H/k^D), \quad \beta = \ln(k^H/k^D)/\ln(k^D/k^T),$$
$$\gamma = \beta + 1 = \ln(k^H/k^T)/\ln(k^D/k^T) \quad (4)$$

For the case where the kinetic isotope effects arise only from differences in zero-point energies between the initial and the transition state, Swain and Schaad[29] have shown for overbarrier reactions at high temperature that $\ln(k^i/k^j) \propto (m_i^{1/2} - m_j^{1/2})$, leading to the values $\alpha = 1.44$, $\beta = 2.27$, and $\gamma = 3.27$. In several theoretical calculations by various authors[29] it turned out that (i) in the case of tunneling of all three isotopes at low temperatures $\alpha > 1.44$, $\beta < 2.27$, and $\gamma < 3.27$, (ii) the Swain−Schaad relations hold at higher temperatures, (iii) $\alpha < 1.44$, $\beta > 2.27$, and $\gamma > 3.27$ when only H tunnels. Therefore, tunneling may be realized even if no deviations from the Swain−Schaad relations are observed.

We found it interesting, therefore, to calculate α and γ from the theoretical Arrhenius curves of Figure 9. The results are indicated in Figure 9c,f together with rectangular bars indicating the temperature ranges where rate constants were available. These bars were included in order to show that this kind of data analysis is not suitable for the cases of porphyrin and its anion, as it requires considerable extrapolations of the calculated Arrhenius curves, which depend very much on the tunneling model used. Nevertheless, the plot shows the expected deviations from the Swain−Schaad relations at low temperatures but only small deviations around room temperature where tunneling is still the important reaction pathway for H.

Conclusions

We have shown that by using strong phosphazene bases it is possible to remove a single proton from porphyrin, leading to the conjugate porphyrin anion, which is subject to a degenerate proton tautomerism in the liquid and the solid state according to Figure 1b. The rate constants are independent of the environment. The kinetic H/D/T isotope effects were measured in a large temperature range, together with those reported previously[4e,7,13] for the corresponding single-proton transfer steps in the parent compound (Figure 1a). The H transfer in the anion is much faster than in the parent compound, in contrast to the

D and T transfers, which are only slightly accelerated. This effect can be qualitatively explained in terms of proton tunneling, which can occur in the anion at much lower energies as compared to the parent compound where proton transfer leads to metastable cis intermediates of higher energy. The results constitute a unique data set of six Arrhenius curves for more or less the same reaction. We hope that these data provide enough information for future testing on improved dynamic theories of high-barrier single-proton transfers in the future.

Acknowledgment. This work was supported by the Deutsche Forschungsgemeinschaft, Bonn-Bad Godesberg, the Freie Universität Berlin, and the Fonds der Chemischen Industrie, Frankfurt. The National Tritium Labeling Facility is supported by the Biomedical Research Technology Program, National Center for Research Resources, U.S. National Institutes of Health, under Grant P41 RR01237, through Contract DE-AC03-76SF00098 with the U.S. Department of Energy. D.E.W. receives continuing support from the U.S. Department of Energy, Office of Energy Research, Office of Health and Environmental Research, Health Effects Research Division, and an instrumentation grant was received from the U.S. National Science Foundation, Grant BBS 87-20134.

Supporting Information Available: Tables of the temperature-dependent coupling constants $^{1}J_{^{1}H-^{15}N}$ and $^{1}J_{^{3}H-^{15}N}$ of porphyrin and its conjugate porphyrin anion and of the ^{1}H NMR chemical shifts of the anion used for the line shape analyses (3 pages). Ordering information is given on any current masthead page.

JA961313Q